Phonon renormalization from local and transitive electron-lattice couplings in strongly correlated systems

E. von Oelsen,[1] A. Di Ciolo,[2] J. Lorenzana,[2,3] G. Seibold,[1] and M. Grilli[2]
[1]*Institut für Physik, BTU Cottbus, P.O. Box 101344, 03013 Cottbus, Germany*
[2]*SMC-INFM-CNR, Dipartimento di Fisica, Università di Roma "La Sapienza," P. Aldo Moro 2, 00185 Roma, Italy*
[3]*ISC-CNR, Via dei Taurini 19, 00185 Roma, Italy*
(Received 29 October 2009; revised manuscript received 19 March 2010; published 21 April 2010)

Within the time-dependent Gutzwiller approximation applied to one-dimensional Holstein and Su-Schrieffer-Heeger-Hubbard models, we study the influence of electron correlations on the phonon self-energy. For the local Holstein coupling, we find that the phonon-frequency renormalization gets weakened upon increasing the on-site interaction U for all momenta. In contrast, correlations can enhance the phonon-frequency shift for small wave vectors in the Su-Schrieffer-Heeger-Hubbard model. Moreover, the time-dependent Gutzwiller approximation applied to the latter model provides a mechanism which leads to phonon-frequency corrections at intermediate momenta due to the coupling with double-occupancy fluctuations. Both models display a shift of the nesting induced to a $q=0$ instability when the on-site interaction becomes sufficiently strong and thus establishing phase separation as a generic phenomenon of strongly correlated electron-phonon coupled systems.

DOI: 10.1103/PhysRevB.81.155116 PACS number(s): 71.10.Fd, 71.38.−k, 74.72.−h

I. INTRODUCTION

Transition-metal compounds are usually characterized by strong electron-electron and electron-phonon interactions (for an overview cf. Ref. 1). The interplay of these interactions can give rise to a large variety of interesting electronic properties which also reflect in the energy and momentum structure of the phonons. In this regard, a well-known phenomenon is the occurrence of bond-stretching phonon anomalies which are observed in high-T_c cuprates $La_{2-x}Sr_xCuO_4$ (LSCO, Refs. 2 and 3) and $YBa_2Cu_3O_{6+x}$,[4] $HgBa_2CuO_{4+\delta}$,[5] $Nd_{1.86}Ce_{0.14}CuO_{4+\delta}$,[6] $Bi_2Sr_{1.6}La_{0.4}Cu_2O_{6+\delta}$ (Ref. 7) but also in Pb- and K-doped $BaBiO_3$,[8] Sr_2RuO_4,[9] $La_{1.69}Sr_{0.31}NiO_4$,[10] and $La_{1-x}Sr_xMnO_3$.[11]

The interpretation of such experiments requires an understanding of the renormalization of phonons in a strongly correlated electron system which is the purpose of the present paper. Such an analysis is usually based on Hubbard-type models and the implementation of the electron-lattice coupling is possible via the dependency of on-site energies and of hopping integrals as a function of some atomic coordinates. There are two generic one-dimensional (1D) models which allow for a separate consideration of both couplings. In the first case, where one restricts to the interaction between electron density and coordinate of the same lattice site, the coupling is usually termed a Holstein or molecular crystal model.[12] In the second case, when the hopping between nearest-neighbor sites is expanded in terms of the positions of these sites, the resulting electron-lattice coupling is often named after Su, Schrieffer, and Heeger (SSH) who have used this type of interaction for the analysis of solitons in polyacetylene.[13]

Since lattice vibrations are partially screened by the electrons, the latter can have a profound influence on the effective dispersion of the phonons. One example is the Kohn anomaly[14] caused by the abrupt change in electronic screening near wave vectors $\mathbf{q}$ which are twice the Fermi momentum k_F (nesting). Moreover, electronic correlations alter the electron dynamics of the system and thus also affect the phonon dispersion. In the case of a Holstein coupling, correlations suppress charge fluctuations (and the related e-ph coupling) at large momenta $q\sim 2k_F$ more than at low momenta $q\sim 0$. Thus it has been shown[15,16] that the formation of a charge-density wave (CDW) is suppressed in favor of a phase-separation instability. For the phonons, this has the immediate consequence that the dispersion anomaly is shifted from the Kohn anomaly wave vector $q=2k_F$ to $q=0$.

Naturally the interplay between lattice and electronic degrees of freedom has already been investigated by means of several techniques. Some of the approaches, such as quantum Monte Carlo (QMC),[17–23] exact diagonalization,[24–27] and dynamical mean-field theory[28–34] are intrinsically nonperturbative but are numerically challenging and suffer some limitations (small lattice sizes, no momentum resolution, etc.). On the other hand, (semi)analytical approaches such as variational ones, slave boson, and large-N expansion[15,35–44] deal with infinite systems but within approximate treatments. It should be noticed that most of the work has been done on the Hubbard-Holstein model. The papers which explicitly deal with an Hubbard-SSH model[18,22,35,36,39,40] mainly focus on the interplay between correlations and dimerization or superconductivity, respectively. Little has been said on the renormalization of the electron-phonon coupling and its momentum dependence in this case, which is the problem which we address.

In this paper, we want to study the correlation effects on the phonon excitations for both Holstein and SSH models on the same footing. To this aim, we need a method which is not numerically very demanding but still provides a quantitatively acceptable treatment of the strongly correlated regime. In this regard, we find the Gutzwiller approximation (GA) supplemented with random-phase approximation (RPA)-type fluctuations, the so-called time-dependent GA (TDGA), a good compromise. This technique corresponds to Vollhardt's

Fermi-liquid (FL) approach[45] with the fluctuations extended to finite frequencies and momenta. Electron-phonon interactions will be treated in the Born-Oppenheimer approximation.

It is worth mentioning that the TDGA approach has been tested in various situations and found to be accurate compared with exact diagonalization.[46–49] Computations for realistic models have provided a description of different physical quantities in agreement with experiment.[50–52]

In the discussion of results, we will restrict to one-dimensional systems. This clearly simplifies the computations and the presentation of the results. It has the drawback that strictly one-dimensional systems are those for which our Fermi-liquid-like approach is expected to be less suited. Thus our results should not be taken too literally in this case. On the other hand, the qualitative behavior we find is rather independent of dimension. For example, for the Holstein model, we find here the same qualitative behavior for the charge response as we have found before in larger dimensions.[53] Despite the inadequacy of a Fermi-liquid treatment for strictly one-dimensional systems, several real systems are only quasi-one-dimensional and in those cases, our computations can be applicable. We also found that in certain filling ranges the results are surprisingly accurate.

The scheme of our paper is as follows. In Sec. II, we define the model and show how the Hubbard-Holstein and SSH Hamiltonians are represented within the GA. After introducing the TDGA in Sec. II C, the phonon self-energy for both Holstein and SSH couplings is derived in Secs. II D and II E. In Secs. III A and III B, we present the results for the phonon self-energies of the Holstein and SSH-Hubbard models, respectively. Our conclusions can be found in Sec. IV and details of our calculations are given in the Appendix A. In Appendix B, we provide specific comparisons of our results with exact and Monte Carlo results in one dimension.

II. FORMALISM

A. Model

Our investigations are based on the following Hamiltonian:

$$H = H_e + H_{e\text{-}ph} + H_{ph}, \tag{1}$$

where H_e denotes the Hubbard model, $H_{e\text{-}ph}$ the coupling between electrons and phonons, and H_{ph} the bare phonon part.

Here we restrict to one-dimensional systems and consider for the electronic part hopping between nearest neighbors,

$$H_e = -t\sum_{i,\sigma}(c^\dagger_{i,\sigma}c_{i+1,\sigma} + c^\dagger_{i+1,\sigma}c_{i,\sigma}) + U\sum_i n_{i,\uparrow}n_{i,\downarrow}, \tag{2}$$

where $c^{(\dagger)}_{i,\sigma}$ destroys (creates) an electron on lattice site R_i and $n_{i,\sigma}=c^\dagger_{i,\sigma}c_{i,\sigma}$.

We consider two types of electron-phonon coupling. The first is a local Holstein interaction initially motivated from a molecular crystal model,

$$H^{hol}_{e\text{-}ph} = -\alpha\sum_{i,\sigma} u_i(n_{i,\sigma} - \langle n_{i,\sigma}\rangle), \tag{3}$$

where u_i is the coordinate of an internal mode of the molecules affecting the site energy at site i. Its dynamics is described by

$$H^{hol}_{ph} = \frac{1}{2}K\sum_i u_i^2 + \frac{1}{2M}\sum_i p_i^2 \tag{4}$$

and corresponds to dispersionless phonons. Here K and M denote elastic constant and reduced mass and p_i are the conjugate momenta at site i.

The second type of coupling originates from the dependence of the electronic hopping on the atomic coordinates. For the one-dimensional model under consideration, this so-called SSH or Peierls interaction is given by

$$H^{\mathrm{SSH}}_{e\text{-}ph} = -\alpha t\sum_{i,\sigma}(u_{i+1}-u_i)(c^\dagger_{i,\sigma}c_{i+1,\sigma} + c^\dagger_{i+1,\sigma}c_{i,\sigma}) \tag{5}$$

and in this case, the lattice dynamics is determined from

$$H^{\mathrm{SSH}}_{ph} = \frac{1}{2}K\sum_i (u_{i+1}-u_i)^2 + \frac{1}{2M}\sum_i p_i^2. \tag{6}$$

The parameter $\alpha<0$ is the logarithmic derivative of the hopping integral with respect to the interatomic distance. We fix the lattice space $a=1$.

B. Gutzwiller approximation

We treat the model Eq. (1) within the GA supplemented by Gaussian fluctuations, the evaluation of which are outlined in the next section. The GA can either be motivated from a slave-boson approach[54] or a variational ansatz formally evaluated in infinite dimensions.[55,56] The variational wave function is given by $|\Psi\rangle=\hat{P}|\phi\rangle$, where the Gutzwiller projector $\hat{P}$ acts on the Slater determinant $|\phi\rangle$. This approach incorporates the correlation-induced renormalization of the kinetic energy and treats the Hubbard on-site interaction via the variational double-occupancy parameters D_i. For each term in the Hamiltonian, we derive an energy functional $E^{\mathrm{GA}}[\rho,D]\equiv\langle\Psi|H|\Psi\rangle$, where we have introduced the one-body density matrix associated with the Slater determinant $\rho_{i,j,\sigma}=\langle\phi|c^\dagger_{i,\sigma}c_{j,\sigma}|\phi\rangle$. Specifically the energy functional for the electronic part Eq. (2) reads as

$$E^{\mathrm{GA}}_e[\rho,D] = -t\sum_{i,\sigma} z_{i,\sigma}z_{i+1,\sigma}(\rho_{i,i+1,\sigma}+\rho_{i+1,i,\sigma}) + U\sum_i D_i \tag{7}$$

and the z factors are given by

$$z_{i\sigma} = \frac{\sqrt{(\rho_{ii,\sigma}-D_i)(1-\rho_{ii}+D_i)}+\sqrt{(\rho_{ii,-\sigma}-D_i)D_i}}{\sqrt{\rho_{ii,\sigma}(1-\rho_{ii,\sigma})}}. \tag{8}$$

Further on, $\rho_{ij}=\Sigma_\sigma\rho_{ij,\sigma}$.

Within the Born-Oppenheimer approximation, the electronic expectation value of $H_{e\text{-}ph}$ determines the lattice potential. In contrast to the local Holstein coupling, for elec-

tronic degrees, the transitive SSH electron-phonon interaction Eq. (5) is also renormalized by the z factors and the corresponding energy functional reads as

$$E_{e\text{-}ph}^{\mathrm{SSH,GA}} = -\alpha t \sum_{i,\sigma} (u_{i+1} - u_i) z_{i,\sigma} z_{i+1,\sigma} \times (\rho_{i,i+1,\sigma} + \rho_{i+1,i,\sigma}). \tag{9}$$

The GA variational ground state is then obtained upon minimizing E^{GA} with respect to $\{D\}$, $\{u\}$, and ρ under the constraint that the latter derives from a Slater determinant, i.e., $\rho^2=\rho$. In the following, our starting point will be an homogeneous state. The formation of possible charge-density wave (in case of the Holstein model) and dimerized (in case of the SSH model) states will appear as instabilities of the homogeneous state. Thus our initial ground state is characterized by $u_i \equiv 0$, $\rho_{ii,\sigma} \equiv \rho_0/2$, $D_i \equiv D_0$, and $z_i \equiv z_0$. The ground-state energy per site is therefore simply determined from Eq. (7) and reads

$$E^{\mathrm{GA}}[\rho, D]/N = z_0^2 e_0 + U D_0 \tag{10}$$

and e_0 denotes the energy per site of a noninteracting system with charge density ρ_0. For later use, we also denote the critical value of the on-site repulsion $U=U_c=32t/\pi$ for a half-filled one-dimensional chain at which the Brinkman-Rice (BR) transition (i.e., complete localization of the charge carriers with $D_0=0$) takes place.

C. Time-dependent Gutzwiller approximation

In order to study fluctuations beyond the GA saddle-point solution, necessary for the evaluation of the phonon self-energies, we use the time-dependent GA which has been developed in Refs. 46 and 47.

We briefly illustrate the formalism for the electronic part H_e and further on show how lattice fluctuations can be implemented into the theory. Further details can be found in Refs. 46, 47, and 53.

We study the response of the system to a small time-dependent external field which produces time-dependent fluctuations in the density matrix $\delta\rho$ and the double-occupancy δD. This can then be obtained by expanding E^{GA} up to quadratic order in the density and double-occupancy fluctuations $\delta\rho$ and δD.

For a translationally invariant ground state, it is convenient to perform the expansion in momentum space. Besides the local fluctuation $\delta\rho_{\mathbf{q}}$, we introduce the bond charge fluctuation,[53]

$$\delta T_i = -t \sum_{\sigma\eta=\pm 1} (\delta\rho_{i+\eta,i,\sigma} + \delta\rho_{i,i+\eta,\sigma}).$$

It is convenient to introduce the hopping factor in the definition of δT_i so that it can also be interpreted as a local kinetic energy. Notice however that the z factors are omitted. The Fourier transform is given by

$$\delta T_q = -2t \sum_{k,\sigma} [\cos(k+q) + \cos(k)] \delta\rho_{k+q,k,\sigma}. \tag{11}$$

For later use it is also convenient to introduce the antisymmetric combination of bond charge fluctuations,

$$\delta T_i^- = -t \sum_{\sigma\eta=\pm 1} \eta(\delta\rho_{i+\eta,i,\sigma} + \delta\rho_{i,i+\eta,\sigma}).$$

with Fourier transform,

$$\delta T_q^- = -2it \sum_{k,\sigma} [\sin(k+q) - \sin(k)] \delta\rho_{k+q,k,\sigma}. \tag{12}$$

It is easy to check that the two fluctuations are related by a function of q,

$$\delta T_q^- = i \tan\left(\frac{q}{2}\right) \delta T_q. \tag{13}$$

The second-order energy expansion in the charge channel of Eq. (7) follows as

$$E_e^{\mathrm{GA},(2)} = \frac{1}{N}\left[\frac{1}{2}\sum_q V_q \delta\rho_q \delta\rho_{-q} + z_0 z_D' \sum_q \delta D_q \delta T_{-q} + \frac{1}{2} z_0 (z' + z'_{+-}) \sum_q \delta\rho_q \delta T_{-q} + \sum_q L_q \delta\rho_q \delta D_{-q} + \frac{1}{2}\sum_q U_q \delta D_q \delta D_{-q}\right] \tag{14}$$

with the following definitions:

$$V_q = \frac{e_0 z_0}{2}(z''_{++} + 2z''_{+-} + z''_{--}) + \frac{1}{2}(z' + z'_{+-})^2 e_0 \cos(q),$$

$$L_q = e_0 z_0 (z''_{+D} + z''_{-D}) + z'_D (z' + z'_{+-}) e_0 \cos(q),$$

$$U_q = 2e_0 z_0 z''_D + 2(z'_D)^2 e_0 \cos(q),$$

where z' and z'' denote derivatives of the hopping factors which are given in the Appendix A.

The double-occupancy fluctuations can be expressed in terms of the density fluctuations by use of the antiadiabaticity condition which assumes that the double occupancy adjusts to the instantaneous configuration of the charge,[46]

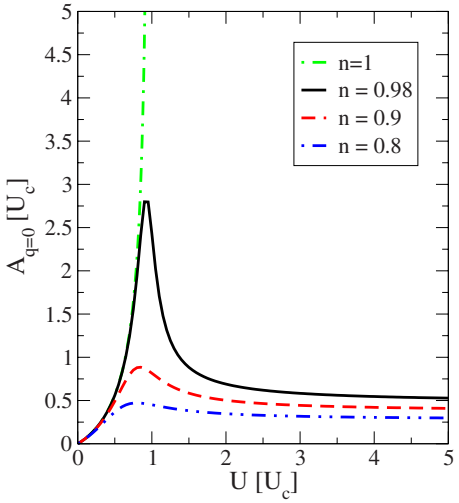

FIG. 1. (Color online) The interaction coefficient $A_{q=0}$ for various values of particle density n in units of the Brinkman-Rice critical on-site repulsion U_c for a one-dimensional chain.

$$\frac{\partial E_e^{\mathrm{GA},(2)}}{\partial \delta D_q} = 0 \tag{15}$$

and one obtains the following functional which only depends on the local and intersite charge deviations,

$$E_e^{\mathrm{GA},(2)} = \frac{1}{2N}\sum_q \begin{pmatrix} \delta\rho_q & \delta T_q \end{pmatrix} \begin{pmatrix} A_q & B_q \\ B_q^* & C_q \end{pmatrix} \begin{pmatrix} \delta\rho_{-q} \\ \delta T_{-q} \end{pmatrix}, \tag{16}$$

where

$$\underline{\underline{W_q^{e\text{-}e}}} = \begin{pmatrix} A_q & B_q \\ B_q^* & C_q \end{pmatrix} \tag{17}$$

is the interaction kernel. The elements of $\underline{\underline{W_q^{e\text{-}e}}}$ are given by

$$A_q = V_q - \frac{L_q^2}{U_q},$$

$$B_q = \frac{1}{2} z_0 \left(z' + z'_{+-} - z'_D \frac{2L_q}{U_q} \right),$$

$$C_q = -4\frac{(z_0 z'_D)^2}{U_q}\cos^2(q/2), \tag{18}$$

and the long-wavelength limit of the Eq. (11) element $A_{q=0}$, which dominates the interaction kernel close to half filling is shown in Fig. 1. For small U, one finds $A_{q=0} \approx U/2$ whereas $A_{q=0}$ is enhanced close to the Brinkmann-Rice transition $U = U_c$. At exactly half filling, one finds

$$A_q = \frac{U(U_c + U)(U - 2U_c)}{4U_c(U - U_c)} \tag{19}$$

for $U < U_c$.

Since the energy expansion in Eq. (16) is a quadratic form in $\delta\rho_q$ and δT_q [see also Eq. (11)], it is useful to introduce the following susceptibility matrix for the noninteracting system χ_q^0:

$$\underline{\underline{\chi_q^0}}(\omega) = \frac{1}{N}\sum_{k\sigma} \begin{pmatrix} 1 & -2t[\cos(k) + \cos(k+q)] \\ -2t[\cos(k) + \cos(k+q)] & 4t^2[\cos(k) + \cos(k+q)]^2 \end{pmatrix} \frac{n_{k+q,\sigma} - n_{k\sigma}}{\omega + \epsilon_{k+q} - \epsilon_k - i0^+}. \tag{20}$$

The susceptibility for the interacting system is then obtained from the following RPA series:

$$\underline{\chi_q} = \underline{\underline{\chi_q^0}} + \underline{\underline{\chi_q^0}}\,\underline{\underline{W_q^{e\text{-}e}}}\,\underline{\chi_q}, \tag{21}$$

where the element $(\chi_q)_{11}$ corresponds to the correlation function for the local charge response.

D. Phonon self-energy for the Holstein coupling

As mentioned above, due to the local nature of the Holstein coupling Eq. (3), it is not renormalized by the z factors and thus its quadratic contribution to the energy expansion is given by

$$E_{e\text{-}ph}^{hol,(2)} = -\alpha\frac{1}{N}\sum_q Q_{-q}\delta\rho_q, \tag{22}$$

where $Q_q = \Sigma_i \exp(-iqR_i)u_i$ denotes the Fourier-transformed (normal) coordinate fluctuation (remember that the saddle-point solution has $u_i = u_0 = 0$ so that we can skip the δ symbol).

Similarly we write the lattice energy Eq. (4) as

$$E_{ph}^{hol,(2)} = \frac{1}{2N}\sum_q \left\{ \frac{P_q P_{-q}}{M} + M\Omega^2 Q_q Q_{-q} \right\} \tag{23}$$

with $\Omega^2 = K/M$.

The small time-dependent deviation from the electronic ground state $\delta\rho_q$ will act as a force on the lattice coordinates via $E_{e\text{-}ph}^{hol,(2)}$ and the corresponding equation of motion reads

$$M\ddot{Q}_q + M\Omega_q^2 Q_q = -N\frac{\partial E_{e\text{-}ph}^{hol,(2)}}{\partial Q_{-q}} = \alpha\delta\rho_q. \tag{24}$$

As a consequence, the lattice vibrations are shifted to new frequencies ω_q which depend on the electronic charge fluctuation $\delta\rho_q$,

$$(\omega_q^2 - \Omega^2)Q_q = -\frac{\alpha}{M}\delta\rho_q. \tag{25}$$

On the other hand, $\delta\rho_q$ can be determined from linear-response theory when we view Eq. (22) as a small perturbation on the electronic system. With the charge susceptibility derived in the previous section, one has

$$\delta\rho_q = (\chi_q)_{11}(-\alpha Q_q) \tag{26}$$

which upon inserting in Eq. (25) yields

$$\omega_q^2 = \Omega^2 + \frac{\alpha^2}{M}(\chi_q)_{11} \equiv \Omega^2 + 2\Omega\Sigma_q, \tag{27}$$

where Σ_q denotes the phonon self-energy. In these equations, $\chi_q(\omega)$ and $\Sigma_q(\omega)$ should be evaluated at $\omega = \omega_q$. Since the phonon dynamics is assumed to be much slower than the electron dynamics, it is a good approximation to evaluate the susceptibilities in the static limit.

We see that in the case of the Holstein coupling, the phonon-frequency shift is solely determined by the local charge susceptibility renormalized by electronic correlations within the GA. For later use, we define the ratio between self-energies in the correlated and uncorrelated case,

$$\Gamma_q \equiv \frac{\Sigma_q(U)}{\Sigma_q(U=0)} \tag{28}$$

which for the Holstein coupling becomes

$$\Gamma_q = \frac{(\chi_q)_{11}}{(\chi_q^0)_{11}}. \tag{29}$$

In addition, it is convenient to introduce the following coupling constant which has energy units:

$$g_{hol} = \alpha \sqrt{\frac{1}{2M\Omega}} \tag{30}$$

so that the phonon self-energy for the Holstein model is given by

$$\Sigma_q = g_{hol}^2 (\chi_q)_{11}. \tag{31}$$

E. Phonon self-energy for the SSH coupling

The case of the SSH electron-lattice coupling is more subtle since the interaction energy Eq. (9) depends on the z factors, the fluctuations of which we have to consider in the evaluation of Σ_q.

Expansion of Eq. (9) up to second order in the fluctuating fields yields for the Fourier-transformed effective electron-lattice interaction,

$$E_{e\text{-}ph}^{\mathrm{SSH},(2)} = \alpha z_0^2 \frac{1}{N}\sum_q \delta T_q^- Q_{-q} + i\alpha e_0 z_0 (z' + z'_{+-}) \times \frac{1}{N}\sum_q \sin(q)\,\delta\rho_q Q_{-q} + 2i\alpha e_0 z_0 z'_D \frac{1}{N}\sum_q \sin(q)\,\delta D_q Q_{-q} \tag{32}$$

with the same definitions already introduced in Sec. II C. Besides the coupling to the transitive fluctuations δT_q, the correlations induce a coupling of the lattice to local density ($\delta\rho_q$) and double-occupancy (δD_q) fluctuations. Unlike the Holstein case, the antiadiabaticity condition now includes the electron-lattice coupling Eq. (32) in addition to the bare electronic part Eq. (15),

$$\frac{\partial[E_e^{\mathrm{GA},(2)} + E_{ph}^{\mathrm{SSH},(2)}]}{\partial\,\delta D_q} = 0 \tag{33}$$

so that the double-occupancy fluctuations can be expressed via the density *and* lattice fluctuations,

$$\delta D_q = 2i\alpha z_0 z'_D \frac{\sin(q)}{U_q} Q_q - \frac{L_q}{U_q}\delta\rho_q - \frac{z_0 z'_D}{U_q}\delta T_q. \tag{34}$$

Inserting Eq. (34) into Eqs. (14) and (32) and including also the (Fourier transformed) lattice part Eq. (6) yields

$$E_{tot}^{\mathrm{SSH},(2)} = E_e^{\mathrm{GA},(2)} + E_{e\text{-}ph}^{\mathrm{SSH},(2)} + E_{ph}^{\mathrm{SSH},(2)}, \tag{35}$$

where $E_e^{\mathrm{GA},(2)}$ was derived in Sec. II C, Eq. (16). The effective coupling of the lattice to the electronic-density fluctuations is given by

$$E_{e\text{-}ph}^{\mathrm{SSH},(2)} = \alpha\frac{1}{N}\sum_q W_q^1 \delta\rho_q Q_{-q} + \alpha\frac{1}{N}\sum_q W_q^2 \delta T_q Q_{-q}, \tag{36}$$

where we used Eq. (13) to eliminate the antisymmetric fluctuations and introduced the elements of the vector $\mathbf{W}_{\mathbf{q}}^{el\text{-}ph}$,

$$W_q^1 = ie_0 z_0 \sin(q)\left[z' + z'_{+-} - 2z'_D\frac{L_q}{U_q}\right],$$

$$W_q^2 = iz_0^2\tan(q/2) - 2ie_0(z_0 z'_D)^2\frac{\sin(q)}{U_q}. \tag{37}$$

The lattice part becomes

$$E_{ph}^{\mathrm{SSH},(2)} = \frac{1}{2N}\sum_q \left\{\frac{P_q P_{-q}}{2M} + M\Omega_q^2 Q_q Q_{-q}\right\}. \tag{38}$$

Interestingly, the elimination of the double-occupancy introduces a novel renormalization of the phonon dispersion,

$$\Omega_q^2 = 2\frac{K}{M}[1-\cos(q)] - \frac{1}{M}(2\alpha e_0 z_0 z'_D)^2\frac{\sin^2(q)}{U_q}. \tag{39}$$

The (squared) dispersion is composed of the acoustic branch $\sim 1-\cos(q)$ of the uncorrelated atomic chain and a contribution which arises from the double-occupancy fluctuations. We will show below that it induces a phonon softening in addition to the contribution which comes from electronic screening.

The phonon self-energy in the present case can be derived via a similar procedure as before, taking into account the vectorial character of the susceptibility, and reads,

$$\Sigma_q = g_q^2[\mathbf{W}_{\mathbf{q}}^{el\text{-}ph}]^T \underline{\underline{\chi_q}}\,\mathbf{W}_{-\mathbf{q}}^{el\text{-}ph} \tag{40}$$

where the electronic susceptibility matrix $\underline{\underline{\chi_q}}$ is obtained from Eq. (21). We also defined the dimensionless coupling constant,

$$g_q = \sqrt{\frac{\tilde{g}}{\hbar\Omega_q}}, \tag{41}$$

$$\tilde{g} = \alpha^2\frac{\hbar^2}{2M}. \tag{42}$$

In the uncorrelated limit $U=0$, the self-energy reduces to

$$\Sigma_q(U=0) = 4g_q^2(U=0)\sin^2(q/2)(\chi_q^0)_{22}, \tag{43}$$

where the coupling constant Eq. (41) has to be evaluated with the bare acoustic dispersion $\Omega_q^2(U=0) = 2\frac{K}{M}[1-\cos(q)]$.

Finally, it should be noted that the parameters of the problem are given by $\hbar\omega_0 \equiv \sqrt{K/M}$, $\tilde{g}$ and U measured in units of the hopping $t \equiv 1$ unless otherwise specified and we set $\hbar \equiv 1$ in the following.

III. RESULTS

A. Holstein coupling

The Holstein case has been analyzed in higher dimension in Ref. 53. As a reference for the new SSH results and to

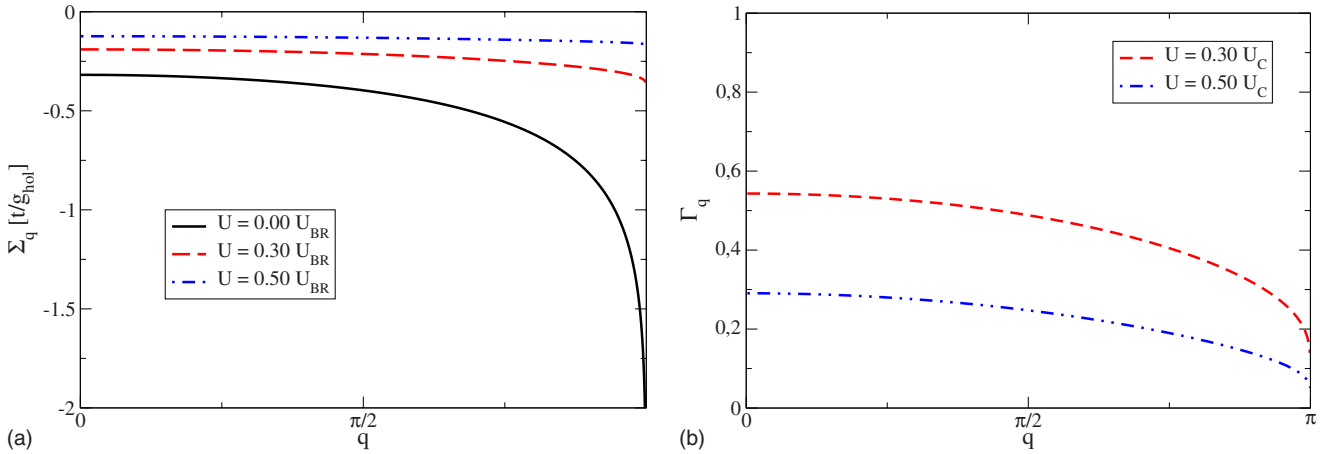

FIG. 2. (Color online) (a) Self-energy Σ_q in units of t/g_{hol} and (b) ratio between correlated and uncorrelated self-energies Γ_q for the half-filled Holstein-Hubbard model as a function of momentum q.

unify the language, we present here the analogous results in 1D which are qualitatively similar to the ones in higher dimensions. A more detailed analysis and comparison with QMC results in one dimension can be found in Appendix B.

The (static) phonon self-energy for the Holstein coupling $\Sigma_q^{hol} \equiv \Sigma_q^{hol}(\omega=0) = g_{hol}^2[\chi_q]_{11}(\omega=0)$ corresponds to the local charge correlation so that the discussion of the previous section directly applies also here. Figure 2(a) shows Σ_q^{hol} for the half-filled system where it is given by

$$\Sigma_q^{hol} = g_{hol}^2 \frac{[\chi_q^0]_{11}}{1 - A_q[\chi_q^0]_{11}}.$$

The primary purpose of these results is to illustrate the generic behavior expected in higher dimensions rather than to comprise the physics of 1D systems.

Due to the divergency of $[\chi_q^0]_{11}$ at $q=2k_F=\pi$, the corresponding singularity in Σ_q^{hol} gets suppressed upon increasing U. This suppression persists for all momenta which can also be seen from the vertex Γ_q, Fig. 2(b), cf. Eq. (28) which quantifies the phonon-frequency shift for the correlated system as compared to the noninteracting case,

$$\Gamma_q = \frac{1}{1 - A_q[\chi_q^0]_{11}}. \tag{44}$$

In the limit $q \to 0$, where $(-\chi_q^0)_{11}$ equals the density of states $N(E_F)$ the reduction in $\Gamma_{q=0}$ is therefore determined by the effective interaction A_q which diverges for U approaching the Brinkmann-Rice transition (and thus $\Gamma_q \to 0$). On the other hand, at $q=\pi$, the local noninteracting charge correlations $(\chi_{q=\pi}^0)_{11}$ display a divergence due to nesting and are thus responsible for the vanishing of $\Gamma_{q\to\pi}$ in this limit.

At finite doping [Fig. 3(a)], the singularity of Σ_q^{hol} at $U=0$ occurs at $q=2k_F<\pi$ and similarly to the half-filled system it becomes suppressed upon increasing U. As discussed in Appendix A (cf. Fig. 11), for large on-site interaction U, the charge susceptibility (and thus $|\Sigma_q^{hol}|$) acquires a maximum at small momenta so that the dominant phonon renormalization is shifted from $q=2k_F$ to $q=0$. On the other hand [Fig. 3(b)], the reduction in Γ_q is still most pronounced at the Fermi momenta $q=2k_F$ where the bare Lindhard susceptibility $(\chi_q^0)_{11}$ logarithmically diverges whereas $\Sigma_{q=2k_F}(U>0)$ stays finite and thus $\Gamma_{q=2k_F}=0$. Of course this is peculiar to

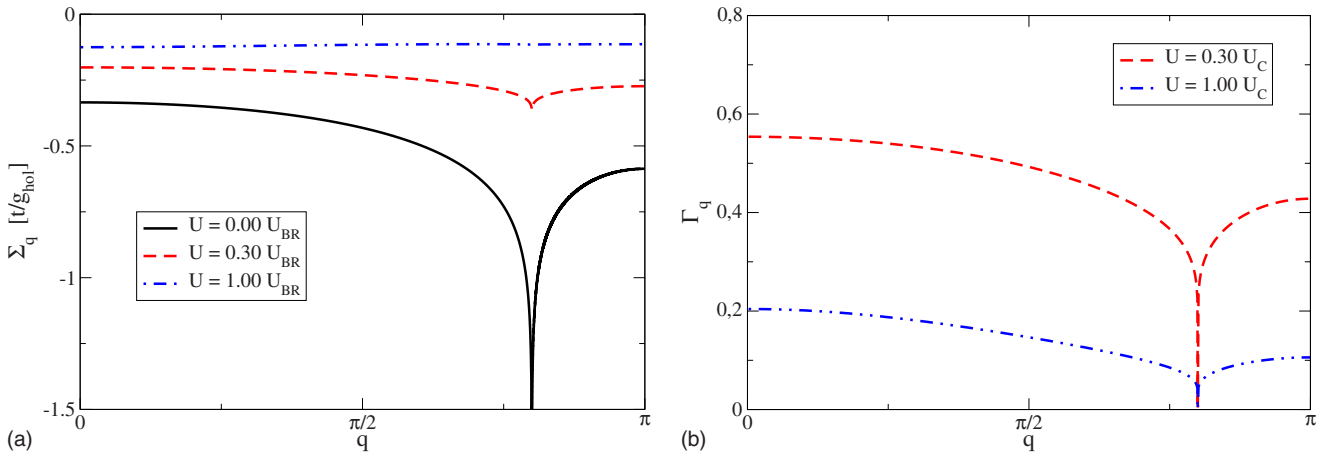

FIG. 3. (Color online) (a) Self-energy Σ_q in units of t/g_{hol} and (b) ratio between correlated and uncorrelated self-energies Γ_q for the Holstein-Hubbard model (particle density $n=0.8$) as a function of momentum q.

the one-dimensional system where one has perfect nesting for each carrier density.

We now analyze in more detail the mode which becomes soft when the dominating instability shifts from $q=2k_F$ to $q=0$ for large U and close to half filling. The dressed phonon propagator,

$$D_q(\omega) = \frac{D_q^0(\omega)}{1 - g_{hol}^2[\chi_q]_{11}(\omega)D_q^0(\omega)} \tag{45}$$

couples the Holstein phonon Ω_0 with the energy of the particle-hole excitations $\sim v_\rho q$ when we use the long-wavelength limit for the charge susceptibility given in Eq. (B1). Then $D_q(\omega)$ acquires new poles at

$$\omega_+^2 = \Omega_0^2 + \frac{4g_{hol}^2 v_F}{\pi\Omega_0} q^2, \tag{46}$$

$$\omega_-^2 = (v_\rho q)^2 - \frac{4g_{hol}^2 v_F}{\pi\Omega_0} q^2 \tag{47}$$

corresponding to a hardening of the Holstein phonon and a softening of the effective (zero-sound) particle-hole velocity. Thus the instability at $q=0$ does not follow from a zero in the phonon-type mode but due to the fact that the zero-sound particle-hole excitations acquire an imaginary velocity. Since the poles of the dressed electronic susceptibility are identical to those of $D_q(\omega)$, this also corresponds to a phase-separation instability so that the present approach generalizes the analysis of Refs. 15 and 57 for $U\to\infty$ Hubbard models to finite on-site interactions.

B. SSH coupling

For the transitive electron-phonon coupling, we have seen in Sec. II E that correlations already induce a renormalization of the phonon dispersion Eq. (39),

$$\Omega_q = \sqrt{(\Omega_q^0)^2 - (\Delta\Omega_q)^2} \tag{48}$$

due to the elimination of the double-occupancy fluctuations [cf. Eqs. (33) and (34)]. Here $\Omega_q^0 = 2\omega_0 \sin(q/2)$ denotes the acoustic branch for $U=0$ and the correlation induced contribution $\sim -(\Delta\Omega_q)^2$ is always negative [since $U_q>0$ in Eq. (39)]. The corresponding softening of Ω_q is shown in Fig. 4.

The renormalization vanishes for both $q\to 0$ and $q\to\pi$, and is largest for intermediate momenta $q\sim\pi/2$. This can be understood from Eq. (34) where the first term links the displacements to the double-occupancy fluctuations $\delta D_q \sim \sin(q)/U_q Q_q$. Remember that U_q is the interaction energy of double-occupancy fluctuations [cf. Eq. (7)] which has a significant momentum dependence only close to half filling and large U. Therefore, the spatial relation between Q_q and δD_q is mainly determined by $\sin(q)$ and thus largest at $q \approx \pi/2$. The inset of Fig. 4 depicts the corresponding lattice modulation (horizontal arrows) which, due to the increased (decreased) hybridization, favors a modulation of the density and double occupancies with the same periodicity (vertical arrows).

The correction $(\Delta\Omega_q)^2$ to the phonon dispersion induced by the double-occupancy fluctuations is separately displayed

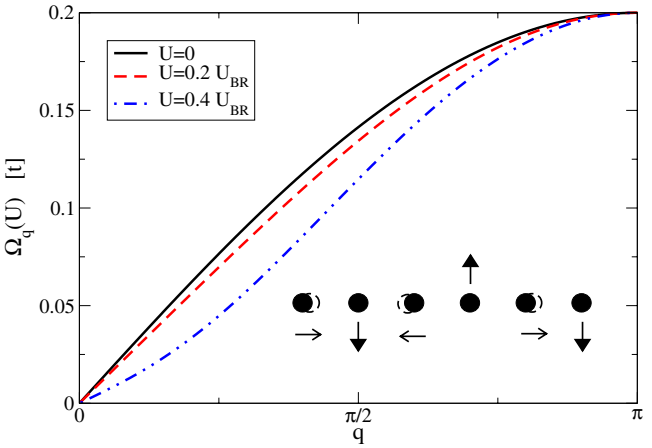

FIG. 4. (Color online) Acoustic-phonon dispersion in the SSH model for three different U values at half filling ($\tilde{g}=0.01$ and $\omega_0=0.1$). Shown is only the influence of the double-occupancy fluctuations on Ω_q. The inset displays atomic displacements with wave vector $q=\pi/2$ (horizontal arrows) and the associated modulation of the double occupancy (vertical arrows) with the same periodicity.

in Fig. 5. For the half-filled system (top panel), the maximum of $(\Delta\Omega_q)^2$ shifts to smaller q values upon increasing U due to the more significant momentum dependence of U_q as mentioned above. This is less pronounced for the doped system (lower panel) where the maximum in the correlation-induced correction stays close to $q=\pi/2$. Note also that $(\Delta\Omega_q)^2$ has a maximum as a function of U. This is due to the fact that the SSH electron-phonon interaction Eq. (9) is renormalized by the z factors which decrease with increasing U so that the transitive fluctuations become suppressed. In this regard, $(\Delta\Omega_q)^2$ results from a subtle interplay of kinetic and correlation effects.

We now turn to the influence of electronic-density fluctuations on the phonon dispersion which is measured in terms of the phonon self-energy Σ_q Eq. (40).

Figure 6(a) displays Σ_q for the half-filled system. In this limit, the local-density fluctuations (originating from the Hubbard interaction) are decoupled from the transitive ones. Therefore, the latter are not screened and the divergence at $q=\pi$ in the case of the SSH coupling is not removed upon increasing U in contrast to the Holstein-Hubbard model. As a consequence, the phonon excitations always (i.e., for infinitesimally small electron-phonon coupling) become unstable for $q=\pi$ corresponding to the dimerized state. Correlations lead to a suppression (enhancement) of Σ_q for large (small) momenta as can be more clearly seen from Fig. 6(b) which shows the ratio $\Gamma_q = \Sigma_q(U)/\Sigma_q(U=0)$. In the limit $q=\pi$, one can show that the ratio is given by $\Gamma_{q=\pi} = z_0^2$, i.e., it is completely determined by the hopping renormalization factors of the GA. This is consistent with the fact, that, for the half-filled dimerized system, correlations suppress the dimerization order parameter[18,35] due to the reduction in the effective electron-phonon coupling.

In the limit $q\to 0$, the self-energy vanishes, however, the slope of $\Sigma_{q\to 0}$ strongly depends on the correlations and leads to the observed increase in $\Gamma_{q\to 0}$ with increasing U [Fig. 6(b)]. The main reason for this enhancement comes from the

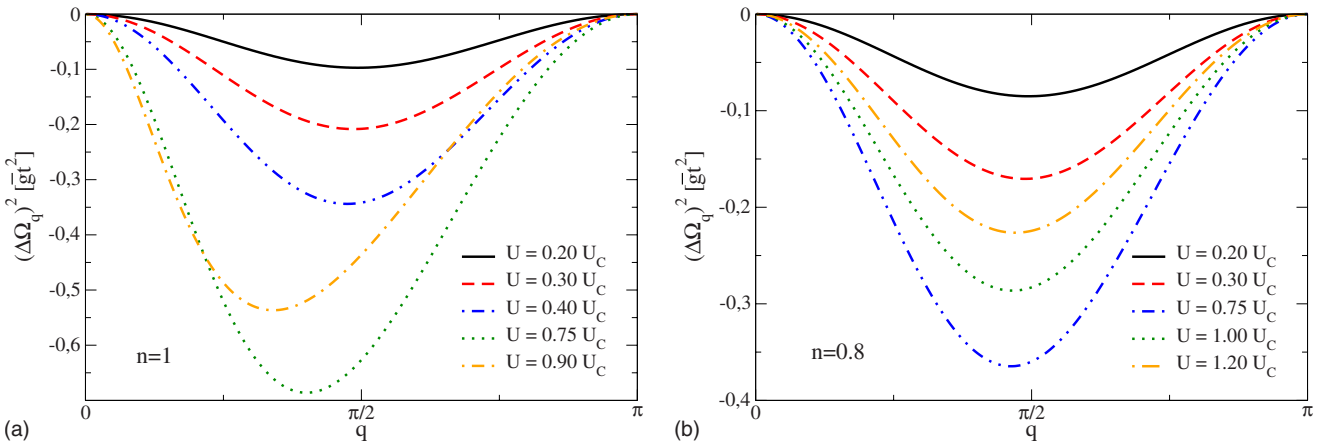

FIG. 5. (Color online) Correlation-induced correction to the phonon dispersion (in units of $\tilde{g}t^2$) from the elimination of double-occupancy fluctuations. Charge densities are $n=1$ [panel (a)] and $n=0.8$ [panel (b)].

fact that the SSH coupling is a coupling to transitive electronic correlations which at half filling and small momenta are decoupled from the local ones. In the limit $q \to 0$ and half filling, Eq. (40) becomes

$$\Sigma_q^{\mathrm{SSH}} \approx g_q^2 |W_q^2|^2 (\chi_q^0)_{22}, \tag{49}$$

$$W_q^2 \approx iq\left[z_0^2 + 2\frac{U^2}{U_c^2}\right] = iq\left[1 + \frac{U^2}{U_c^2}\right] \tag{50}$$

and one finds that Σ_q^{SSH} is not screened by the strong local charge fluctuations. On the contrary, since $(\chi_q^0)_{22} \sim 1/z_0^2$ it becomes enhanced due to the increase in the quasiparticle mass with U. However, for the bare SSH coupling $|W_q^2|^2 = q^2 z_0^4$ this effect would be overcompensated resulting in $\Sigma_q \sim z_0^2$. It is due to the TDGA induced vertex corrections Eq. (50) that the increase in $(\chi_q^0)_{22}$ is even amplified by the concomitant increase in $|W_q^2|^2$ with U. Finally, another (though much weaker) factor which leads to the enhancement of $\Sigma_{q\to 0}^{\mathrm{SSH}}$ with U comes from the dependence of the coupling constant g_q Eq. (41) on the phonon frequencies $g_q \sim 1/\sqrt{\Omega_q}$ which become softened due to the elimination of the double-occupancy fluctuations [cf. Eq. (39)].

The enhancement of the vertex Γ_q at small momentum is a new effect very much in contrast with the result in the Holstein case[53] where one always finds $\Gamma_q < 1$, i.e., a reduction in self-energy corrections with U.

Figure 7 displays the behavior of Σ_q and Γ_q for the doped SSH model. Similar to the case of half filling, Σ_q is reduced upon increasing U for large momenta. However, the behavior for small q becomes more subtle as can be seen from Fig. 7(b). As a function of U, the self-energy $\Sigma_{q\to 0}$ passes through a minimum and for large U exceeds again the uncorrelated value (i.e., $\Gamma_{q\to 0} > 1$) similar to the half-filled case. This behavior results from a subtle interplay between local and transitive charge fluctuations which are now coupled. For small U, the screening induced by the local charge fluctuations leads to a suppression of $(\chi_q)_{22}$ and also Σ_q. Only at larger U, the vertex corrections for $|W_q^2|$ can overcome this decrease and effectively enhance again the self-energy at small momenta.

In contrast to half filling, now the coupling of the local charge-density fluctuations induces the suppression of the $q = 2k_F$ divergence in the self-energy. As in case of the Hol-

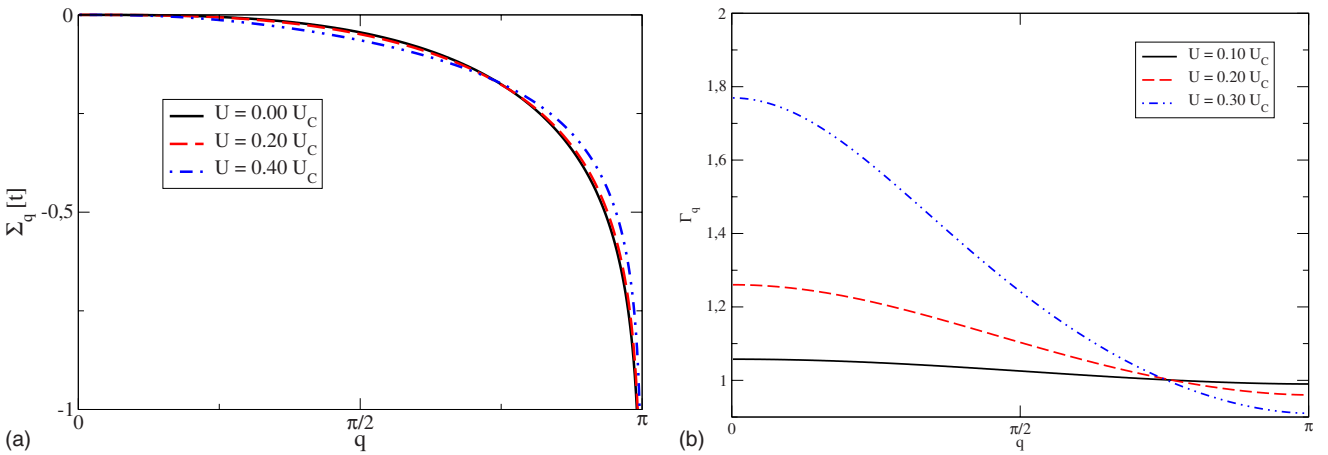

FIG. 6. (Color online) (a) Phonon self-energy Σ_q for the half-filled Hubbard-SSH model and different values of U/U_c. (b) Ratio $\Gamma_q = \Sigma_q(U)/\Sigma_q(U=0)$ for the same system. Parameters: $\tilde{g}=0.01$ and $\omega_0=0.1$.

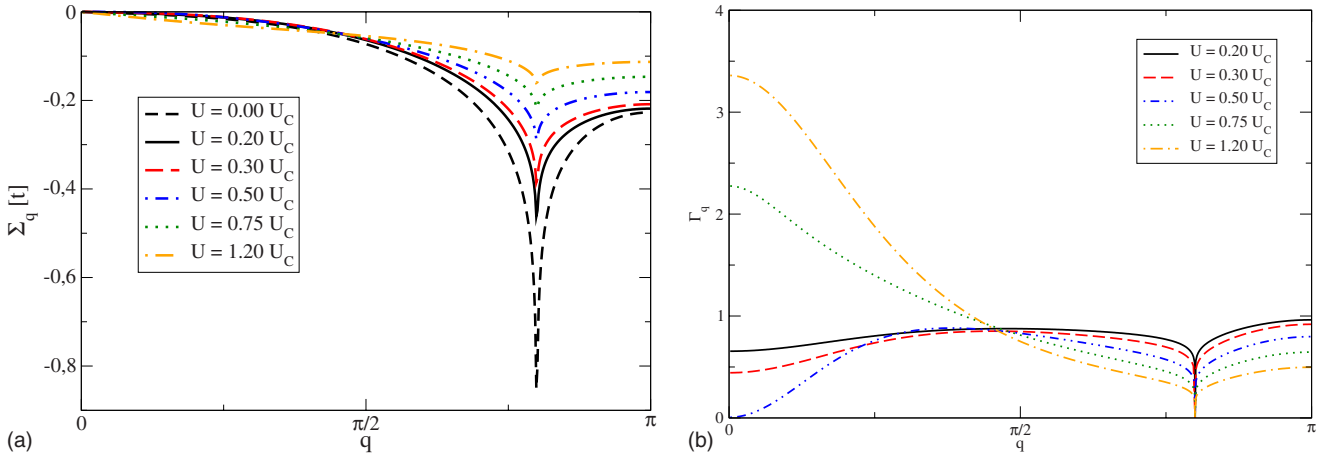

FIG. 7. (Color online) (a) Phonon self-energy Σ_q for the doped ($n=0.8$) Hubbard-SSH model and different values of U/U_C. (b) Ratio $\Gamma_q=\Sigma_q(U)/\Sigma_q(U=0)$ for the same system. Parameters: $\tilde{g}=0.01$ and $\omega_0=0.1$.

stein coupling, one therefore finds that $\Gamma_{q=2k_F}=0$ since $\Sigma_{q=2k_F}(U=0)$ logarithmically diverges whereas $\Sigma_{q=2k_F}(U>0)$ stays finite.

Within the Holstein-Hubbard model, we have seen that away from half filling the maximum self-energy shifts from the nesting vector $q=2k_F$ to $q=0$ when the correlations become sufficiently strong. As a consequence, a large electron-phonon coupling will induce a CDW instability for small U while a phase-separation instability will occur for large U (of course with a dependence on the carrier density). Is there a similar scenario for the transitive coupling in the SSH model? We determine the instabilities from the zero-frequency poles of the phonon propagator,

$$D_q(\omega=0)=\frac{D_q^0(\omega=0)}{1-\Sigma_q D_q^0(\omega=0)} \tag{51}$$

which yields the condition

$$\Omega_q=-2\Sigma_q \tag{52}$$

and Ω_q is the effective phonon dispersion given in Eq. (39). The solid line in Fig. 8 marks the lattice instability at $q=2k_F$, i.e., where the system undergoes a transition toward a combined CDW and bond-order state. This instability is suppressed for large U due to the suppression of the $2k_F$ peak in Σ_q as shown in Fig. 7.

The maximum at $n=0.85$ in the instability line is due the following. At $n=1$, the self-energy can be written as $\Sigma_q(U)=z_0^2\Sigma_q(U=0)$ so that upon approaching half filling the self-energy is determined by both the diverging $\Sigma_q(U=0)$ and the Gutzwiller renormalization factor z_0^2 which at $n=1$ tends to zero for $U>U_c$ (in Fig. 8, the solid bar at $n=1$ indicates this regime where the charge carriers are localized). As a consequence, $|\Sigma_q(U)|$ develops a maximum as a function of concentration and fixed U which is reflected in the maximum of the instability line.

Another instability occurs when the system is stable against nesting (i.e., $|\Sigma_{q=2k_F}|<\Omega_{q=2k_F}/2$) but the slope of $|\Sigma_{q\to 0}|$ becomes larger than the slope of $\Omega_{q\to 0}$. Then there exists another solution of the condition Eq. (52) The transition toward this instability occurs at $q=0$ when both slopes become equal. The corresponding line is shown in Fig. 8 by the dashed-dotted curve. Similar to the Holstein-Hubbard model, we thus find a $q=0$ instability for large U which here is confined to a region close to half filling. However, in contrast to the Holstein model, where the phase separation is due to an instability of the zero-sound collective mode $v_\rho q$ caused by the coupling to the optical phonon, in the SSH model we have a coupling between two acoustic modes, i.e., $\Omega_q\approx v_{ph}q$ and $v_\rho q$. For the situation we have analyzed in Fig. 8, we find always $v_{ph}<v_\rho$ so that the mode which becomes unstable has dominantly phonon character. This phase-separation instability is very different from the one in the Holstein model, specially when the long-range part of the Coulomb interaction is taken into account. In the Holstein model, only molecular modes are allowed, therefore at long scales the ions provide a rigid background of charges which cancels the carriers charge. A macroscopic phase separation

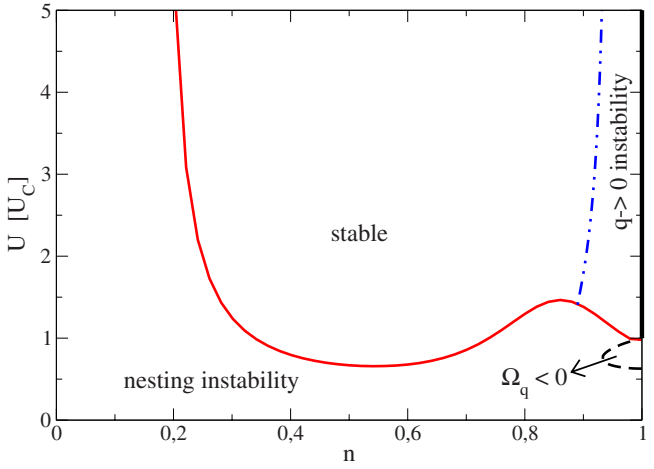

FIG. 8. (Color online) Phase diagram for the SSH model with parameters $\tilde{g}=0.02$ and $\omega_0=0.2$. The solid line indicates the transition to a nesting-induced $q=2k_F$ instability whereas the dashed-dotted line is the $q=0$ instability line. The region enclosed by the dashed line corresponds to the parameter space where $\Omega_q^2<0$ and the bar at $n=1$ indicates the localized regime for $U>U_c$.

of the electronic system is frustrated by this background and in general modulated phases arise.[16,58–63] In the SSH case, the background is allowed to relax at long wavelengths and can follow the charge keeping the system locally neutral. The present instability corresponds therefore to macroscopic phase separation of the solid which in higher dimension is not frustrated by the Coulomb interaction but by elastic effects.[64]

Finally, we have seen that the TDGA applied to the SSH coupling yields an effective phonon dispersion Eq. (39) which yields correlation-induced softening through the elimination of double-occupancy fluctuations (cf. Fig. 5). For large coupling $\tilde{g}$, these frequencies can become complex even without the consideration of density fluctuations. The corresponding regime in Fig. 8 is enclosed by the dashed line. We find (at least for the present model) that this area is always in a parameter regime which corresponds to the nesting-induced instability and therefore never gives rise to a "real" instability.

IV. CONCLUSIONS

We have investigated the renormalization of phonon frequencies within the Hubbard-Holstein and Hubbard-SSH models based on the TDGA approach. Our considerations of the Holstein coupling for one-dimensional correlated systems supplement our investigations in higher dimensions[53] and serve as a reference for our computations of the SSH coupling. In the latter case, we have found that correlations influence the phonon modes Ω_q via two mechanisms. First, the coupling to double-occupancy fluctuations leads to a softening which has a maximum around $q=\pi/2$, depending on U and doping. The second mechanism is the standard screening from density fluctuations. However, in this regard, our TDGA approach goes beyond the standard RPA since it incorporates the interaction between phonons and both, transitive and induced local-density fluctuations. This leads to an interesting dependence of the self-energy Σ_q on the local repulsion U since it becomes suppressed for large but enhanced for small momenta.

We have found that also the transitive coupling of the Hubbard-SSH model gives rise to an interesting phase diagram where correlations can suppress the $q=2k_F$ nesting instability but at the same time are responsible for the occurrence of a $q=0$ instability in the vicinity of half filling. To some extent, our calculations indicate that the phase-separation instability, previously only evidenced for Holstein-type couplings, seems to be a generic property of strongly correlated electrons coupled to phonons. However, in the case of SSH phonons, the phase-separation instability involves the relaxation of the background and corresponds to volume collapse transition close to the Mott insulator, i.e., a transition in which the solid has two possible equilibrium volumes. It is interesting that Mott insulators often show volume instabilities close to the Mott transition consistently with our result.[65]

How do our results apply to higher-dimensional systems, especially with regard to the anomalous softening of bond-stretching modes in perovskite materials?[2–7] Consider, e.g., the half-breathing mode in cuprates which involves the movement of two planar oxygen ions toward the central Cu ion. The induced change in the ionic potential on Cu leads to a Holstein-type coupling whereas the associated modulation of the Cu-O hopping integral gives rise to a coupling of the SSH type. Concerning the latter interaction, it is interesting that the double-occupancy-induced renormalization in the two-dimensional three-band model would lead to a maximum frequency shift at the zone boundary (in contrast to that at $q=\pi/2$ in the 1D SHH model). This kind of interaction therefore induces a downward dispersion of the half-breathing mode which in the lowest approximation just vibrates at constant frequency. Obviously, in order to account for the doping dependence of the softening, one has additionally to consider the effect of the density fluctuations entering the phonon self-energy. In this regard, it would be interesting to investigate whether our approach can improve related Hartree-Fock (HF) calculations within the three-band model[66] which give a too small doping dependence of the softening. In fact, since the correlation functions in the TDGA incorporate the correlation-induced reduction in the kinetic energy, its dependence on the charge-carrier concentration is expected to be much more pronounced than in the HF approach. It should be noted that calculations of the density response for the tJ model also indicate a strong renormalization of bond-stretching phonons[67] with a larger anomaly occurring for half breathing as compared to full-breathing modes.[68]

Our theory can be easily extended toward ground states which break translational symmetry. In this regard, it would be interesting to evaluate the phonon renormalization from striped ground states since there is experimental evidence[69,70] that these textures contribute to the anomalous phonon softening at intermediate q values in high-temperature superconductors. Since codoped LSCO compounds, where static stripe order is unambiguously established, show a rather strong renormalization it has been argued[71] that the corresponding phonon dispersion exhibits a Kohn-type anomaly originating from the $q=2k_F=\pi/2$ scattering along the half-filled stripes. Since the GA (in contrast to HF) leads to half-filled stripes as stable mean-field solutions of the Hubbard model,[50] our approach allows for a test of this scenario from a realistic model.

An interesting question is whether phonon-induced superconductivity can be enhanced by correlations. In the case of Holstein phonons, the increase on the density of states due to correlation is compensated by the vertex corrections so the Hubbard U does not enhance the phonon-induced superconducting instability. This is because the Holstein attractive interaction and the Hubbard repulsive interaction compete on the same charge fluctuation channel. Capone and co-workers[72,73] have shown that the situation is dramatically different when Cooper pairing occurs in a channel that does not involve the same charge fluctuations that are suppressed by U. Our results show some analogy with this work in that we obtain a suppression of the electron-phonon coupling in the Holstein case and an enhancement in the SSH case where the bond fluctuations induced by the phonons are not in direct competition with the charge fluctuations suppressed by U. An analogous enhancement of superconductivity may also

work in the correlated SSH model. However, this issue is much more involved since the investigation of pair-pair scattering requires a GA energy functional which is charge-rotationally invariant[74] also for the transitive electron-phonon coupling Eq. (9). As a consequence, the coupling between pair and lattice fluctuations will in general be different from $\mathbf{W}_{\mathbf{q}}^{el\text{-}ph}$ given in Eqs. (37) and (38) and will be considered elsewhere.

ACKNOWLEDGMENTS

We are grateful to Bob Markiewicz for enlightenment comments. E.v.O., M.G., J.L., and G.S. acknowledge financial support from the Vigoni foundation. J.L. thanks KITP-UCSB for hospitality under the program The Physics of Higher Temperature Superconductivity and for partial support from NSF under Grant No. PHY05-51164 at KITP. M.G. and J.L. acknowledge financial support from the MIUR PRIN 2007 (Protest No. 2007FW3MJX003).

APPENDIX A: DEFINITION OF z FACTORS AND DERIVATIVES

In the TDGA expansion, Eq. (14), we have introduced the following abbreviations for the z factors and its derivatives:

$$z_{i\sigma} \equiv z_0, \frac{\partial z_{i\sigma}}{\partial \rho_{ii\sigma}} \equiv z',$$

$$\frac{\partial z_{i\sigma}}{\partial \rho_{ii-\sigma}} \equiv z'_{+-}, \frac{\partial z_{i\sigma}}{\partial D_i} \equiv z'_D,$$

$$\frac{\partial^2 z_{i\sigma}}{\partial \rho_{ii\sigma}^2} \equiv z''_{++}, \frac{\partial^2 z_{i\sigma}}{\partial \rho_{ii\sigma} \partial \rho_{ii-\sigma}} \equiv z''_{+-}, \frac{\partial^2 z_{i\sigma}}{\partial \rho_{ii-\sigma}^2} \equiv z''_{--},$$

$$\frac{\partial^2 z_{i\sigma}}{\partial D_i^2} \equiv z''_D, \frac{\partial^2 z_{i\sigma}}{\partial \rho_{ii\sigma} \partial D_i} \equiv z''_{+D}, \frac{\partial^2 z_{i\sigma}}{\partial \rho_{ii-\sigma} \partial D_i} \equiv z''_{-D}.$$

For the half-filled paramagnetic state, we have $z'=z'_{+-}$ and $z''_{+D}=z''_{-D}$.

APPENDIX B: PROPERTIES OF THE TDGA AND COMPARISON WITH EXACT RESULTS

For simplicity, we have restricted to 1D systems, although our primary interest is higher dimensions. Still it is interesting to analyze to what extent the results are applicable to real 1D or quasi-1D systems by comparing with exact results.

Since in the Holstein case, the phonon self-energies are completely determined by the charge susceptibility $(\chi_q)_{11}$, we first analyze the corresponding TDGA result which for small wave vectors q and close to half filling can be expanded as

$$(\chi_q)_{11} \approx \frac{2}{\pi} \frac{v_F q^2}{\omega^2 - (v_\rho q)^2}, \tag{B1}$$

where $v_F=v_F^0 z_\sigma^2$ is the quasiparticle Fermi velocity and $v_\rho = v_F\sqrt{1+4A_0/(\pi v_F)}$ is the velocity of the (quasi)particle-hole excitations with $A_0 \equiv A_{q=0}$ defined in Eq. (18). The compressibility $\kappa=-(\chi_{q\to 0})_{11}(\omega=0)$ follows as

$$\kappa = \frac{2v_F}{\pi v_\rho^2} = \frac{2}{\pi} \frac{1}{v_F + 4A_0/\pi}. \tag{B2}$$

In the weak-coupling limit, this expression coincides with the perturbative expressions for the Tomonoga-Luttinger liquid.[75] As in the exact case, the effective interaction and the Fermi velocity gets renormalized upon increasing U.

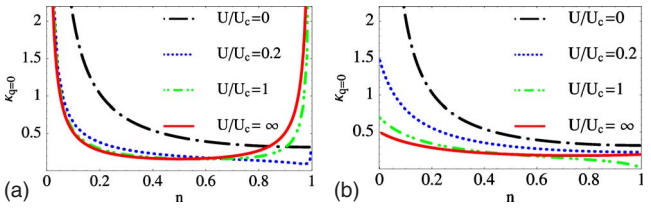

FIG. 9. (Color online) 1D charge compressibility as a function of n and for different values of U/U_c calculated with the Bethe ansatz—exact 1D solution (a) and with the TDGA (b). Here $U_c=32t/\pi$ is the Coulomb repulsion at which the Brinkman-Rice transition takes place for $n=1$ in the GA. In the exact solution, the metal-insulator transition occurs at $U=0$ therefore $U_c=32t/\pi$ is used only as an energy unit.

In Fig. 9, we compare the TDGA charge compressibility with the exact 1D solution of the Hubbard model.[76–78] The renormalization of v_F and the effective interaction pushes the qualitative agreement with exact results to larger values of U than the traditional HF+RPA approach. Strong differences arise close to $n=1$. As soon as the interaction is switched on, the exact compressibility diverges. This can be understood in the strong-coupling limit where the charge degrees of freedom can be mapped to a spinless fermion model[79] and the compressibility is related to the spinless density of states which has a 1D Van Hove divergence. In contrast, the GA yields a compressibility which tends to zero at the BR point. We remark that the GA compressibility has a jump discontinuity for $n=1$ and $U>U_c$. In fact, its left and right limits are finite while its value computed in $n=1$ is zero. At half filling, an antiferromagnetic (AF) broken-symmetry TDGA computation instead of the present paramagnetic one yields much more accurate results.[46]

In the dilute limit, the exact compressibility diverges again whereas the TDGA result yields a finite value. This disagreement is not surprising since the RPA in general is well known to fail at low densities. In this case, a particle-particle approach, recently implemented on top of the GA,[49] would be more appropriate.

Despite the (expected) failure of the paramagnetic TDGA at low and half filling at intermediate fillings, the behavior of the compressibility as a function of U is qualitatively and to some extent quantitatively reproduced. One should keep in mind again that we are using a Fermi-liquid approach whereas the real ground state is a Luttinger liquid.

In Fig. 10, we compare the TDGA charge susceptibility with QMC results from Hirsch and Scalapino.[17,19] Since their data are for $n=0.6$, we expect the TDGA to give reasonable results. Although our formalism is at $T=0$ and the QMC

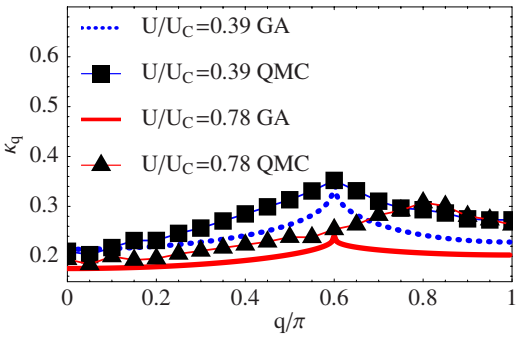

FIG. 10. (Color online) 1D charge susceptibility ($n=0.6$) as a function of q/π: comparison between TDGA and QMC results (Ref. 19).

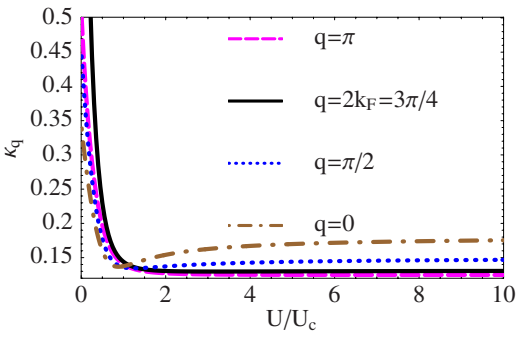

FIG. 11. (Color online) 1D charge susceptibility as a function of U/U_c for $n=0.75$.

study at $T\neq 0$, the comparison is meaningful because their results are at $T=0.0690$, quite low if compared to the electronic energy scales. The QMC susceptibilities generally agree with ours within 10–20 % deviations, and with larger deviations at large momenta for $U\sim U_c$. For large U, in fact, the QMC data exhibit the transfer of the peak from $q=2k_F$ to $q=4k_F$, signature of the spin-charge separation of the 1D Luttinger liquid, clearly absent in our 1D FL. The QMC curves present a finite-T effect that smoothes the peak.

The above results indicate that our FL scheme works quantitatively rather well away from half filling (where an AF TDGA computation would do a better job) and provides reasonable momentum dependencies (but for the subtle Luttinger $4k_F$ peak shift for large U).

In Fig. 11, we show the charge susceptibility κ_q as a function of U/U_c. These results should be taken with a pinch of salt due to the explained drawbacks, however they illustrate well the general behavior of the TDGA that are found in higher dimension.[53] For small deviations of the density from half filling, the compressibility has a minimum close to $U=U_c$ which is due to the corresponding maximum in the Eq. (11) element of the interaction kernel (cf. Fig. 1). For large q, this minimum becomes too shallow to be clearly seen in Fig. 11. At small momenta, the charge susceptibility is close to the compressibility. As the momentum approaches $q=2k_F=n\pi$, the charge susceptibility diverges for small U. However, this divergence is strongly suppressed upon increasing U. At small doping, κ_q is finite but still shows a shallow minimum close to $U=U_c$. This behavior is due to the proximity of the Mott phase which is more clear in higher dimensions.[53] The essential point is that the maximum charge response changes from the wave vector $q=2k_F$ to $q=0$ upon increasing U. Therefore, correlations suppress the nesting-induced transition to a CDW state in favor of phase separation as is discussed in higher-dimensional systems in Ref. 53.

It is important to notice that the failures of the TDGA found at high filling in our comparison with the exact results can be traced back to specific features of the 1D physics (such as, e.g., the spin-charge separation, the equivalence to spinless fermions at $U=\infty$). Therefore, these failures should not be attributed to the TDGA per se but to the underlying assumption of a FL ground state. This is why our results not only provide qualitative informations on the 1D case but also shed light on the physics of the FL state occurring at higher dimensions.

[1] S. Maekawa, T. Tohyama, S. E. Barnes, S. Ishihara, W. Koshibae, and G. Khaliullin, *Physics of Transition Metal Oxides* (Springer, New York, 2004).

[2] R. J. McQueeney, Y. Petrov, T. Egami, M. Yethiraj, G. Shirane, and Y. Endoh, Phys. Rev. Lett. **82**, 628 (1999).

[3] L. Pintschovius and M. Braden, Phys. Rev. B **60**, R15039 (1999).

[4] W. Reichardt, J. Low Temp. Phys. **105**, 807 (1996).

[5] H. Uchiyama, A. Q. R. Baron, S. Tsutsui, Y. Tanaka, W.-Z. Hu, A. Yamamoto, S. Tajima, and Y. Endoh, Phys. Rev. Lett. **92**, 197005 (2004).

[6] M. d'Astuto, P. K. Mang, P. Giura, A. Shukla, P. Ghigna, A. Mirone, M. Braden, M. Greven, M. Krisch, and F. Sette, Phys. Rev. Lett. **88**, 167002 (2002).

[7] J. Graf, M. d'Astuto, C. Jozwiak, D. R. Garcia, N. L. Saini, M. Krisch, K. Ikeuchi, A. Q. R. Baron, H. Eisaki, and A. Lanzara, Phys. Rev. Lett. **100**, 227002 (2008).

[8] M. Braden, W. Reichardt, S. Shiryaev, and S. N. Barilo, Physica C **378-381**, 89 (2002).

[9] M. Braden, W. Reichardt, Y. Sidis, Z. Mao, and Y. Maeno, Phys. Rev. B **76**, 014505 (2007).

[10] J. M. Tranquada, K. Nakajima, M. Braden, L. Pintschovius, and R. J. McQueeney, Phys. Rev. Lett. **88**, 075505 (2002).

[11] W. Reichardt and M. Braden, Physica B **263-264**, 416 (1999).

[12] T. Holstein, Ann. Phys. (N.Y.) **8**, 325 (1959).

[13] W. P. Su, J. R. Schrieffer, and A. J. Heeger, Phys. Rev. **22**, 2099 (1980).

[14] W. Kohn, Phys. Rev. Lett. **2**, 393 (1959).

[15] M. Grilli and C. Castellani, Phys. Rev. B **50**, 16880 (1994).

[16] C. Castellani, C. Di Castro, and M. Grilli, Phys. Rev. Lett. **75**, 4650 (1995).

[17] J. E. Hirsch and D. J. Scalapino, Phys. Rev. Lett. **50**, 1168 (1983).

[18] J. E. Hirsch, Phys. Rev. Lett. **51**, 296 (1983).

[19] J. E. Hirsch and D. J. Scalapino, Phys. Rev. B **29**, 5554 (1984).
[20] J. E. Hirsch, Phys. Rev. B **31**, 6022 (1985).
[21] E. Berger P. Valášek, and W. von der Linden, Phys. Rev. B **52**, 4806 (1995).
[22] B. Srinivasan and S. Ramesesha, Phys. Rev. B **57**, 8927 (1998).
[23] Z. B. Huang, W. Hanke, E. Arrigoni, and D. J. Scalapino, Phys. Rev. B **68**, 220507(R) (2003).
[24] A. Dobry, A. Greco, J. Lorenzana, and J. Riera, Phys. Rev. B **49**, 505 (1994).
[25] A. Dobry, A. Greco, J. Lorenzana, J. Riera, and H. T. Diep, Europhys. Lett. **27**, 617 (1994).
[26] J. Lorenzana and A. Dobry, Phys. Rev. B **50**, 16094 (1994).
[27] See, e.g., M. Capone, M. Grilli, and W. Stephan, Eur. Phys. J. B **11**, 551 (1999), and references therein.
[28] J. K. Freericks and M. Jarrell, Phys. Rev. Lett. **75**, 2570 (1995).
[29] M. Capone, G. Sangiovanni, C. Castellani, C. Di Castro, and M. Grilli, Phys. Rev. Lett. **92**, 106401 (2004).
[30] W. Koller D. Meyer, Y. Ōno, and A. C. Hewson, Europhys. Lett. **66**, 559 (2004).
[31] W. Koller, D. Meyer, and A. C. Hewson, Phys. Rev. B **70**, 155103 (2004).
[32] G. S. Jeon, T. H. Park, J. H. Han, H. C. Lee, and H. Y. Choi, Phys. Rev. B **70**, 125114 (2004).
[33] G. Sangiovanni, M. Capone, C. Castellani, and M. Grilli, Phys. Rev. Lett. **94**, 026401 (2005).
[34] G. Sangiovanni, M. Capone, and C. Castellani, Phys. Rev. B **73**, 165123 (2006).
[35] D. Baeriswyl and K. Maki, Phys. Rev. B **31**, 6633 (1985).
[36] J. H. Kim and Z. Tešanović, Phys. Rev. Lett. **71**, 4218 (1993).
[37] J. Keller, C. E. Leal, and F. Forsthofer, Physica B **206-207**, 739 (1995).
[38] M. L. Kulić and R. Zeyher, Phys. Rev. B **49**, 4395 (1994); R. Zeyher and M. L. Kulić, *ibid.* **53**, 2850 (1996).
[39] B. J. Alder, K. J. Runge, and R. T. Scalettar, Phys. Rev. Lett. **79**, 3022 (1997).
[40] S. Caprara, M. Avignon, and O. Navarro, Phys. Rev. B **61**, 15667 (2000).
[41] E. Koch and R. Zeyher, Phys. Rev. B **70**, 094510 (2004). See also Refs. 16, 17, and 57 therein.
[42] E. Cappelluti, B. Cerruti, and L. Pietronero, Phys. Rev. B **69**, 161101(R) (2004).
[43] R. Citro and M. Marinaro, Eur. Phys. J. B **20**, 343 (2001).
[44] R. Citro, S. Cojocaru, and M. Marinaro, Phys. Rev. B **72**, 115108 (2005).
[45] D. Vollhardt, Rev. Mod. Phys. **56**, 99 (1984).
[46] G. Seibold and J. Lorenzana, Phys. Rev. Lett. **86**, 2605 (2001).
[47] G. Seibold, F. Becca, and J. Lorenzana, Phys. Rev. B **67**, 085108 (2003).
[48] G. Seibold, F. Becca, P. Rubin, and J. Lorenzana, Phys. Rev. B **69**, 155113 (2004).
[49] G. Seibold, F. Becca, and J. Lorenzana, Phys. Rev. Lett. **100**, 016405 (2008).
[50] J. Lorenzana and G. Seibold, Phys. Rev. Lett. **89**, 136401 (2002).
[51] J. Lorenzana and G. Seibold, Phys. Rev. Lett. **90**, 066404 (2003).
[52] G. Seibold and J. Lorenzana, Phys. Rev. Lett. **94**, 107006 (2005).
[53] A. Di Ciolo, J. Lorenzana, M. Grilli, and G. Seibold, Phys. Rev. B **79**, 085101 (2009).
[54] G. Kotliar and A. E. Ruckenstein, Phys. Rev. Lett. **57**, 1362 (1986).
[55] F. Gebhard, Phys. Rev. B **41**, 9452 (1990).
[56] G. D. Mahan, *Many-Particle Physics* (Plenum Press, New York and London, 1990).
[57] F. Becca, M. Tarquini, M. Grilli, and C. Di Castro, Phys. Rev. B **54**, 12443 (1996).
[58] J. Lorenzana, C. Castellani, and C. Di Castro, Phys. Rev. B **64**, 235127 (2001).
[59] J. Lorenzana, C. Castellani, and C. Di Castro, Europhys. Lett. **57**, 704 (2002).
[60] U. Löw, V. J. Emery, K. Fabricius, and S. A. Kivelson, Phys. Rev. Lett. **72**, 1918 (1994).
[61] C. Ortix, J. Lorenzana, and C. Di Castro, Phys. Rev. B **73**, 245117 (2006).
[62] C. Ortix, J. Lorenzana, M. Beccaria, and C. Di Castro, Phys. Rev. B **75**, 195107 (2007).
[63] C. Ortix, J. Lorenzana, and C. Di Castro, Phys. Rev. Lett. **100**, 246402 (2008).
[64] S. Bustingorry, E. A. Jagla, and J. Lorenzana, Acta Mater. **53**, 5183 (2005).
[65] M. Imada, A. Fujimori, and Y. Tokura, Rev. Mod. Phys. **70**, 1039 (1998).
[66] O. Rösch and O. Gunnarsson, Phys. Rev. B **70**, 224518 (2004).
[67] G. Khaliullin and P. Horsch, Phys. Rev. B **54**, R9600 (1996); P. Horsch, G. Khaliullin, and V. Oudovenko, Physica C **341-348**, 117 (2000).
[68] P. Zhang, S. G. Louie, and M. L. Cohen, Phys. Rev. Lett. **98**, 067005 (2007).
[69] D. Reznik, L. Pintschovius, M. Ito, S. Iikubo, M. Sato, H. Goka, M. Fujita, K. Yamada, G. D. Gu, and J. M. Tranquada, Nature (London) **440**, 1170 (2006).
[70] D. Reznik, T. Fukuda, D. Lamago, A. Q. R. Baron, S. Tsutsui, M. Fujita, and K. Yamada, J. Phys. Chem. Solids **69**, 3103 (2008).
[71] S. I. Mukhin, A. Mesaros, J. Zaanen, and F. V. Kusmartsev, Phys. Rev. B **76**, 174521 (2007).
[72] M. Capone, M. Fabrizio, and E. Tosatti, Phys. Rev. Lett. **86**, 5361 (2001).
[73] M. Capone, M. Fabrizio, C. Castellani, and E. Tosatti, Science **296**, 2364 (2002).
[74] G. Seibold, F. Becca, and J. Lorenzana, Phys. Rev. B **78**, 045114 (2008).
[75] J. Voit, Rep. Prog. Phys. **58**, 977 (1995).
[76] E. H. Lieb and F. Y. Wu, Phys. Rev. Lett. **20**, 1445 (1968).
[77] H. Shiba, Phys. Rev. B **6**, 930 (1972).
[78] H. J. Schulz, Phys. Rev. Lett. **64**, 2831 (1990).
[79] M. Ogata and H. Shiba, Phys. Rev. B **41**, 2326 (1990).